A TALE OF TWO DETACHMENTS: STRUCTURAL RELATIONSHIPS AND STRAIN ALONG THE NORTHWEST MARGIN OF THE PIONEER MOUNTAINS METAMORPHIC CORE COMPLEX

James Vogl,[1] Megan Borel,[1] Rory McFadden,[2] and Carolina Ortiz-Guerrero[1]

[1]University of Florida, Gainesville, Florida
[2]Gustavus Adolphus College, St. Peter, Minnesota

INTRODUCTION—GOALS

This field trip explores the geologic relations in the northwestern corner of the Pioneer Mountains metamorphic core complex (fig. 1). Focus will be on the structures and fabrics formed from strain development along two detachments that converge in this area. Taking advantage of the spectacular views, we will also provide overviews of structural relations of the Challis Volcanic Group in the core complex hanging wall and the structural–magmatic relations within the Kane Creek dome in the footwall of the core complex.

For those interested, we will provide a kmz file of the Dover (1983) map of the region. This is no longer available online, but we have the files that we can get to you so that you can use the map in Google Earth on a device in the field. The geologic map of Dover (1983) in various other formats is available at https://ngmdb.usgs.gov/Prodesc/proddesc_9151.htm.

In addition to this field guide, we will provide the link to a virtual field trip using Google Earth. This will allow viewers to explore, from any web browser (cellphone or computer), geological features of the PMCC included in this guide, as well as other important features in additional sites of the core complex that go beyond the scope of our field trip.

GEOLOGIC OVERVIEW

The Pioneer Mountains metamorphic core complex (PMCC) was originally mapped by Dover (1983) as a window of a thrust system, but was later mapped as a metamorphic core complex by Wust (1986). Subsequent work focused on various aspects of the extensional features (O'Neill and Pavlis, 1988; Silverberg, 1990; Vogl and others, 2012; McFadden and others, 2015). The PMCC is bound by the curviplanar Wildhorse detachment on the north, west, and southwest sides and by the White Mountains fault on the east side (fig. 1). In the field trip area, the hanging wall consists of folded, weakly metamorphosed Mississippian Copper Basin Group strata of the Copper Basin thrust plate. On the slopes across the valley to the west of our field trip stops, the hanging wall rocks consist of Devonian–Ordovician rocks (Phi Kappa and Trail Creek Formation) that lie in the hanging wall of the Pioneer thrust fault (which is exposed ~600 m to the west of our stops). Paleozoic rocks are unconformably overlain by Eocene Challis volcanic rocks.

The Wildhorse detachment is largely a top-WNW brittle feature (Wust, 1986; O'Neill and Pavlis, 1988; Silverberg, 1990) that is poorly exposed. The most recent mapping by Diedesch (2011) shows that from the northwestern corner to the southern margins of the complex, the detachment dips 40°–55°, regardless of strike. On the western side of the core complex, the fault zone is characterized as a zone up to 20 m wide of entirely brittle features, including polished/striated surfaces, local hematite-coated surfaces, and chloritic breccias (Diedesch, 2011).

In the field trip area, no slip surfaces are exposed, but fractured Ella marble and Kinnikinic Quartzite occur ~600–700 m SW of stop 4 (fig. 1). The ductile structures within the Wildhorse detachment are best preserved in the Kinnikinic Quartzite, though the Ella marble, granodiorite, and upper paragneiss units display ductile structures as well. Mylonitic foliations dip moderately northwest and quartz stretching lineations plunge shallowly west–northwest. Meter-scale shear bands, asymmetric porphyroclasts of muscovite and feldspar, and S-C structures record top-to-the-NW motion (McFadden and others, 2015). A second region of mylonitic fabrics and asymmetric structures associated with the Wildhorse detachment are preserved within the Middle paragneiss unit ~5 km to the east of the field trip area.

The footwall of the Wildhorse detachment is divided into a middle plate (MP) of metasedimentary units interpreted to correlate with Neoproterozoic–Ordovician rocks (Brennan and others, 2020), and a lower plate (LP; also Wildhorse gneiss complex) consist-

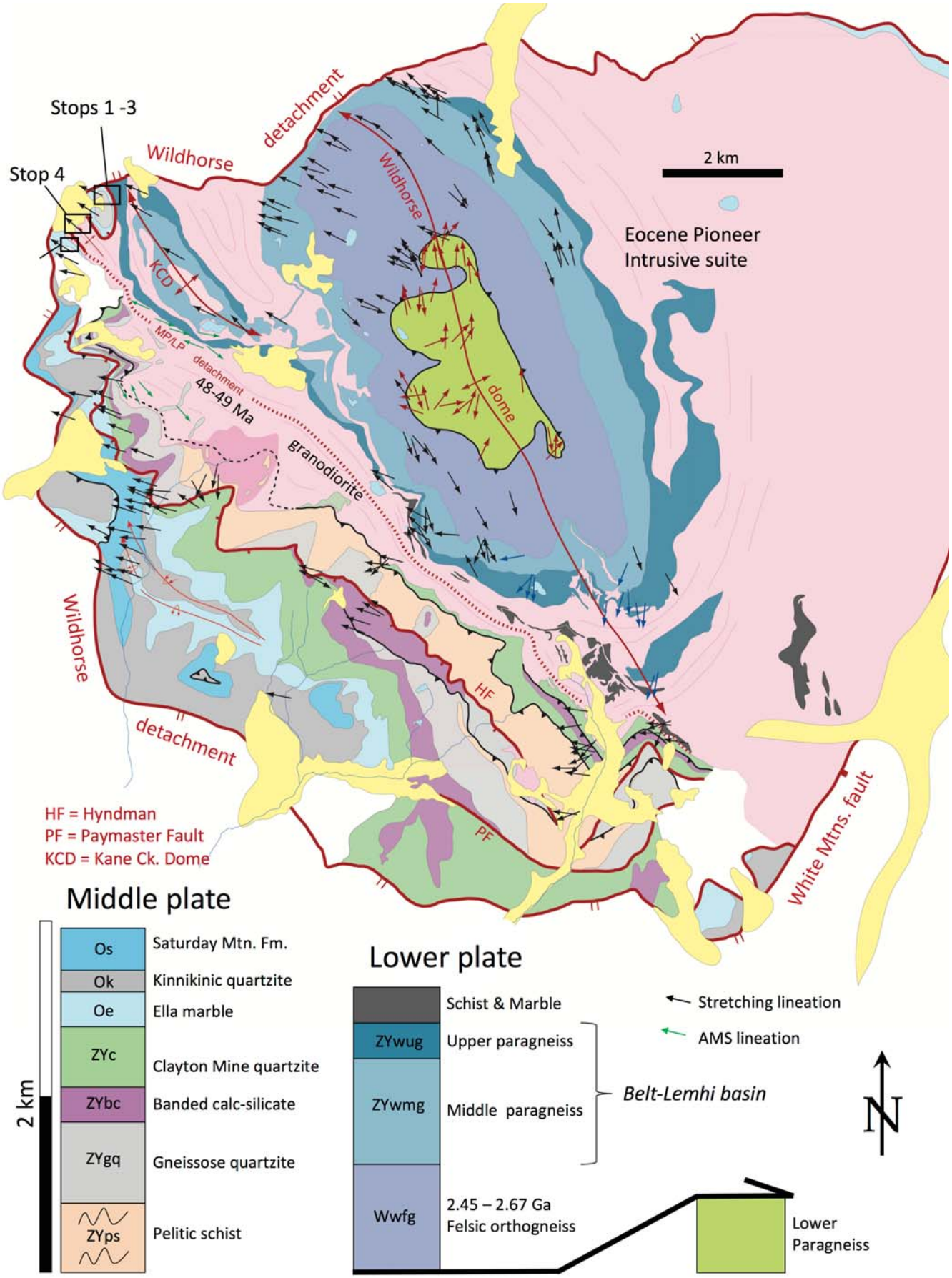

Figure 1. Geologic map of the Pioneer Mountains metamorphic core complex. Contacts are largely from Dover (1983), but all structural data and interpretation of the MP/LP boundary are from our work. Unit names of the lower plate are from Link and others (2017), which are renamed from Dover (1983). Age designations for middle plate units are modified from Dover (1983) based on correlations proposed by Brennan and others (2020).

ing of rocks interpreted to correlate with high-grade Lemhi subbasin rocks of the Belt Supergroup, overlying Neoarchean felsic orthogneiss (Durk-Autenreith, 2007; Cameron, 2010; Link and others, 2017). The footwall is intruded by compositionally diverse (ultramafic to granite) plutonic rocks of the Pioneer intrusive suite. Our dating indicates that the most voluminous phases yield ages of ~50–47 Ma, but small-scale dikes are as young as ~44 Ma (Vogl and others, 2012; and unpublished data from our research team). The lower plate is folded into the elongate NNW-trending Wildhorse dome and the smaller Kane Creek dome (fig. 1).

The MP is cut by several generally SW-dipping faults that were originally interpreted by Dover (1983) as thrust faults. Although a few of these have older on younger relationships and are indeed likely Cretaceous thrust faults, at least two of them (the Paymaster and Hyndman faults; red faults in fig. 1) place younger on older and likely formed (or at least moved) during Eocene extension.

The MP and LP are separated by a granodiorite sheet that has yielded U-Pb zircon ages of 48.6 ± 0.4 Ma and 49.2 ± 0.2 Ma (Vogl and others, 2012; Borel and Vogl, unpublished data). The granodiorite, which appears to be folded around the Wildhorse dome, ranges in thickness from a few hundred meters to just a few meters in the field trip area and at the southern end of the core complex. The granodiorite commonly displays a magmatic foliation, with only weak or localized solid-state fabrics. Mineral lineations as magnetic lineations trend NW and domino boudin trains display a top-NW shear-sense. The entire lower plate stratigraphy is present within/below the granodiorite. However, along the length of the MP/LP boundary, multiple middle plate units are missing and different middle plate units lie directly on the lower plate units (or within the granodiorite; Borel and Vogl, 2020). Thus, we interpret the MP/LP boundary as an extensional detachment (herein the MP/LP detachment; fig. 1) that initiated prior to emplacement of the granodiorite sheet and that motion continued during magmatic injection, but largely ceased following solidification. High-temperature strain in the middle plate units directly overlying the granodiorite suggest that continued top-NW strain was transferred to weaker metasedimentary rocks following solidification of the granodiorite. These relationships will be observed and discussed at the outcrops.

The Wildhorse detachment and MP/LP detachment converge in the area of the field trip (fig. 1). However, to the SW, the ductile strain at the base of the MP diverges from the Wildhorse detachment and the Wildhorse detachment is not associated with ductile fault zone rocks.

The timing of the onset of extension associated with formation of the core complex can only be constrained by the relationships described above in that some extension predates emplacement of the 49–48 Ma granodiorite. Extensive dating of deformed and undeformed dikes throughout the footwall indicates that significant ductile strain accumulated between ~49 and 47 Ma (Vogl and others, 2012; Ortiz-Guerrero and others, 2020) and that some of the middle plate strain above the granodiorite involves ~47 Ma dikes (Vogl and others, 2012). $^{40}Ar/^{39}Ar$ muscovite and biotite cooling ages yield consistent 38–35 Ma ages throughout the footwall (Silverberg, 1990), including 37 Ma ages in the detachment zone at the fieldtrip localities (McFadden and others, 2015). Low-temperature steps from K-feldspar $^{40}Ar/^{39}Ar$ step-heating experiments of Silverberg (1990) give ages around 33 Ma. These data indicate that extension-related exhumation and cooling may have continued into the early Oligocene. We are currently performing additional K-feldspar $^{40}Ar/^{39}Ar$ analysis, including diffusion-domain modeling to better constrain the cooling/exhumation history. Apatite (U-Th)/He dating by Vogl and others (2014) showed that both the footwall and hanging wall to the northwest (Summit Ck. stock) cooled fairly rapidly and simultaneously from ca. 75° beginning ~11 Ma. Vogl and others (2014) suggested that this ca. 2 km of exhumation was related to passage of the Yellowstone hotspot and formation of the eastern Snake River Plain. A range of available geologic constraints suggest between ~12 and 32 km of NW–SE extension after ~48–49 Ma (Vogl and others, 2012).

FIELD TRIP

Getting There

From the intersection of Old Chilly Road and Trail Creek Road, travel roughly southwest for ~19.5 miles (~31.3 km), before turning left (south) on Kane Creek Road (Forestry Road 134). Travel south on Kane Creek Road for ~4.8 mi (~7.7 km) where the road ends at the parking area for the trailhead. Park in designated parking area at coordinates: 43.827300° / -114.175287°. Note: Kane Creek Road is an unim-

proved road and high-clearance vehicles are recommended, but not required. Cars do successfully travel this road. Some sections of the road go through sharp argillites that can be flat tire hazards.

FIELD STOPS

TRAILHEAD PARKING AREA

43.827300°/-114.175287° Elevation ~7,630′

Depart vans on foot and start south down Kane Lake trail. Just before footbridge crossing, head east (right) on Right Fork Kane Creek trail(?). You will gain 300′–400′ of elevation via switchbacks before the trail flattens a bit and turns southwest. The hike between the parking area up until this point is within the quartzite unit (with lesser conglomerate) of the Lower Mississippian Copper Basin Group, whereas the next stretch of the trail goes through the argillite unit of the Copper Basin Group. Dover (1983) mapped the younger argillite unit as occupying the core of a syncline. As we continue on the trail, we will pass through an anticline cored by the quartzite unit before the remaining stretch of trail within the argillite unit. Scattered small outcrops of Copper Basin Group can be found near the trail.

As you continue ~SSW on the trail, across the valley to the west, Dover (1983) mapped the Pioneer thrust fault on the middle to lower slopes. At this location, the fault places Ordovician–Silurian Phi Kappa Formation on top of argillites of the Mississippian Copper Basin Group. In general, the Pioneer thrust fault carries basinal facies eastward over more proximal time-equivalent shallow-water facies (e.g., Kinnikinic Quartzite) and also carries rocks of a Pennsylvanian–Permian basin (Wood River Formation) in its hanging wall. The highest peaks 1.5 to 2 km to the southwest were mapped by Dover (1983) as basal Challis Volcanic Group conglomerates that unconformably overlie Paleozoic rocks.

43.804640°/-114.189347° Elevation ~8850′

After ~3.2 km (2.0 mi) and elevation gain of ~1,200 ft, depart trail and head east to northeast through the open trees and often wet meadows for ~600 m. You will gain ~100′–120′ of elevation before dropping slightly.

We will gather everyone on the crest of the small saddle before dropping down to Stop 1.

STOP 1 43.80564°/-114.18242°

The purpose of this stop is twofold: (1) to provide an overview of geological relations visible from here and (2) to examine exposures of strained Ordovician Kinnikinic Quartzite.

(1) Overviews

Looking east, this location provides outstanding views of the Wildhorse detachment, ridges of Challis volcanics in the hanging wall, and exposures of the Precambrian gneisses and Eocene Pioneer intrusive suite directly across the valley.

In the Kane Creek valley, the Wildhorse detachment fault dips 40°–50° northward. On the eastern side of the valley, chloritized breccia derived from the Precambrian gneisses and/or Eocene intrusive rocks are found within 5–10 m of the projected fault contact, which is within the talus chute. The detachment drops Mississippian Copper Basin Group down against Eocene intrusive rocks of the Pioneer intrusive suite and Precambrian gneisses of the metamorphic core complex's lower plate. Dover (1983) mapped a series of antiforms and synforms in the Copper Basin Group (we walked through the continuation of the northernmost of these on the trail).

The ridge to the north is made of rocks of the Eocene Challis Volcanic Group rock. This section is composed largely of compositionally intermediate lava flows and several sections of epiclastic deposits. From this view, you can see that this section dips moderately to steeply northward. These and other relations in this area will be discussed at the outcrop and additional figures will be shown.

On the prominent ridge to the south of the detachment (footwall), the upper slopes comprise granodiorite and pyroxenite, both part of the Eocene Pioneer intrusive suite. The granodiorite appears to be continuous with those at the field localities observed on this side of the valley. The lower half or so of the slopes are gneisses of the lower plate injected by Eocene intrusions of a variety of scales. The map patterns and foliations broadly define the NW-plunging Kane Creek dome as mapped originally by Dover (1983). The gneisses display a

NW-plunging stretching lineation that is parallel to widespread outcrop-scale folds. Additional relations, including results of recent U-Pb dating, will be discussed at the outcrop.

(2) Kinnikinic Mylonites

The mylonitic Kinnikinic Quartzite is composed of >90% quartz with minor amounts of muscovite and K-feldspar porphyroclasts. The moderately NW-dipping foliation is defined by quartz and muscovite (fig. 2A), and stretched quartz defines a prominent WNW-trending lineation. These mylonitic fabrics are crosscut by prevalent brittle fractures oriented SW–NE (fig. 2B). Asymmetric muscovite fish, sigma-type K-feldspar porphyroclasts, oblique recrystallized quartz foliation, and S-C structures record top-to-the-WNW motion (fig. 2C). Quartzite microstructures near the base and central portion of the section display large, flattened, high-aspect-ratio relict quartz grains, as well as prominent quartz ribbons (fig. 2D). Small, dynamically recrystallized quartz grains are common surrounding the larger grains. Toward the top of the section, quartzites contain prevalent C′-type shear bands with abundant, small recrystallized quartz. Recrystallized quartz grains display an oblique foliation.

From this area, we will walk a few tens of meters to the east going downhill and downsection into the Ella marble.

STOP 2 43.80584°/-114.18184°

Strained Ordovician Ella Marble Section

The Ella marble in the field area consists of forsterite-bearing marble, calc-silicate, and quartzite layers. Original bedding in the marble and calc-silicates is transposed into a foliation with prominent tight to isoclinal and fold hinge lines trending

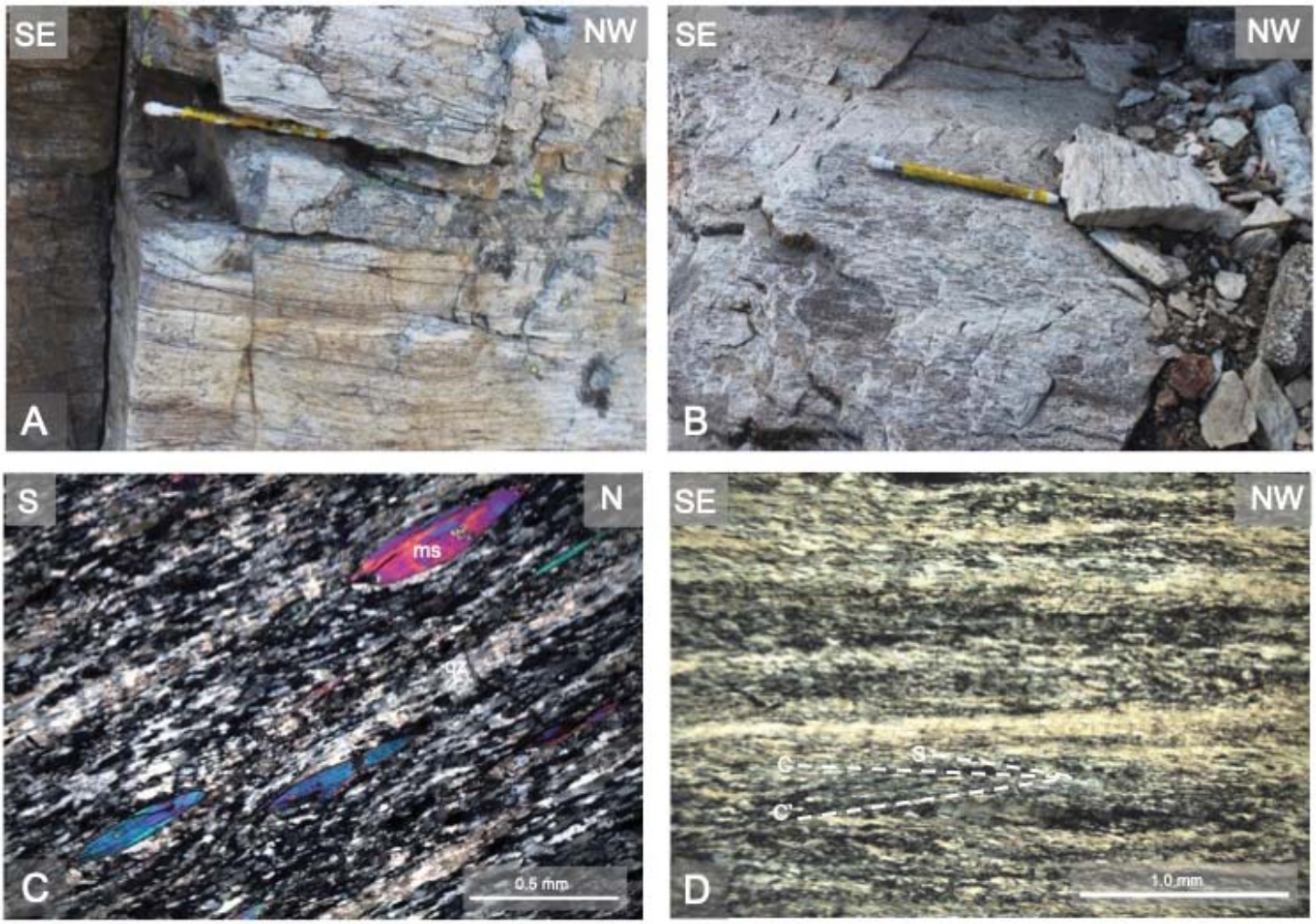

Figure 2. Photos of the Kinnikinic Quartzite found at Stop 1. (A) Mylonitic quartzite with prominent foliation defined by muscovite and quartz. (B) Quartz stretching lineations trending NW crosscut by subvertical brittle fractures. (C) Mylonitic quartzite photo displaying relict quartz grains flattened in foliation and recrystallized quartz with muscovite fish. (D) Mylonitic quartzite photo with quartz ribbons, recrystallized quartz oblique foliation, and S-C-C' structures.

subparallel to the stretching lineation (fig. 3A). Boudins of the underlying granodiorite ranging from centimeter to meter scale are entrained in the marble foliation. Isolated boudins of other felsic intrusive rocks are also common in this section (fig. 3A). These features suggest that the marble records large-magnitude strains. Outcrop-scale, normal-sense, NW-side down shear zones also occur at this locality (fig. 3B).

Continue walking downhill to the east. The MP/LP detachment is exposed along the top of the cliffs. You will need to be careful of the steep drop here!

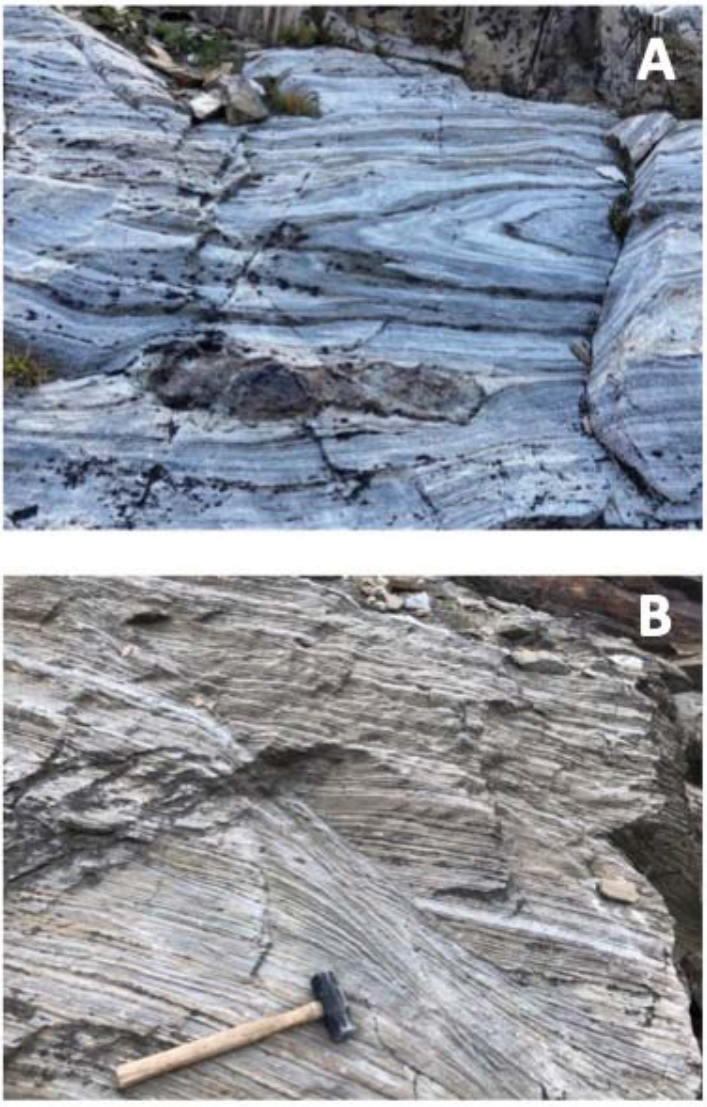

Figure 3. Photos of Ella marble from Stop 2. (A) Field photo of isoclinal folds and boudin with asymmetric strain shadows. (B) Field photo of down-to-NW shear band in layered marbles.

STOP 3 43.805724°/-114.181195°

MP-LP Detachment Zone

Highly strained Ella marbles of Stop 2 are separated from migmatitic Mesoproterozoic upper paragneiss by as little as ~2 m of Eocene granodiorite here, marking the boundary between the middle and lower plates. This juxtaposition indicates that the lowermost four units of the middle plate are missing. However, the Ella–Kinnikinic observed here may be part of a higher thrust sheet. Thus, structural omission may be much greater and include one or more thrust sheets. The Google Earth image in figure 4 provides a broader view of the structural relations in this area.

The upper paragneiss largely exhibits the same high-temperature deformation fabrics as seen in the underlying units and in other parts of the footwall. Evidence for lower temperature ductile deformation, however, is present locally in this area. In some places, the granodiorite is fractured and protomylonitic (fig. 5A), but in others shows little evidence for any significant ductile or brittle strain. In some spots in this area, fine-grained marble mylonites are found directly above the granodiorite. Although the MP/LP boundary zone is not entirely lacking post-intrusion strain, we interpret the juxtaposition of the Ella marble (middle plate) with the upper paragneiss (lower plate) as largely predating intrusion of the granodiorite. This is consistent with the relations along the length of the MP/LP boundary along most of the length to the south (Borel and Vogl, 2020; see above). The Ella marble here contains boudins of the granodiorite (fig. 5B), indicating that the strain was localized in the overlying weak marbles following solidification of the granodiorite. This is also consistent with observations along the MP/LP boundary to the south.

Walk back up over saddle. From the saddle proceed ~650–700 m to the southwest in the meadows and scattered trees. Scramble ~100 vertical feet up the talus slope to outcrop.

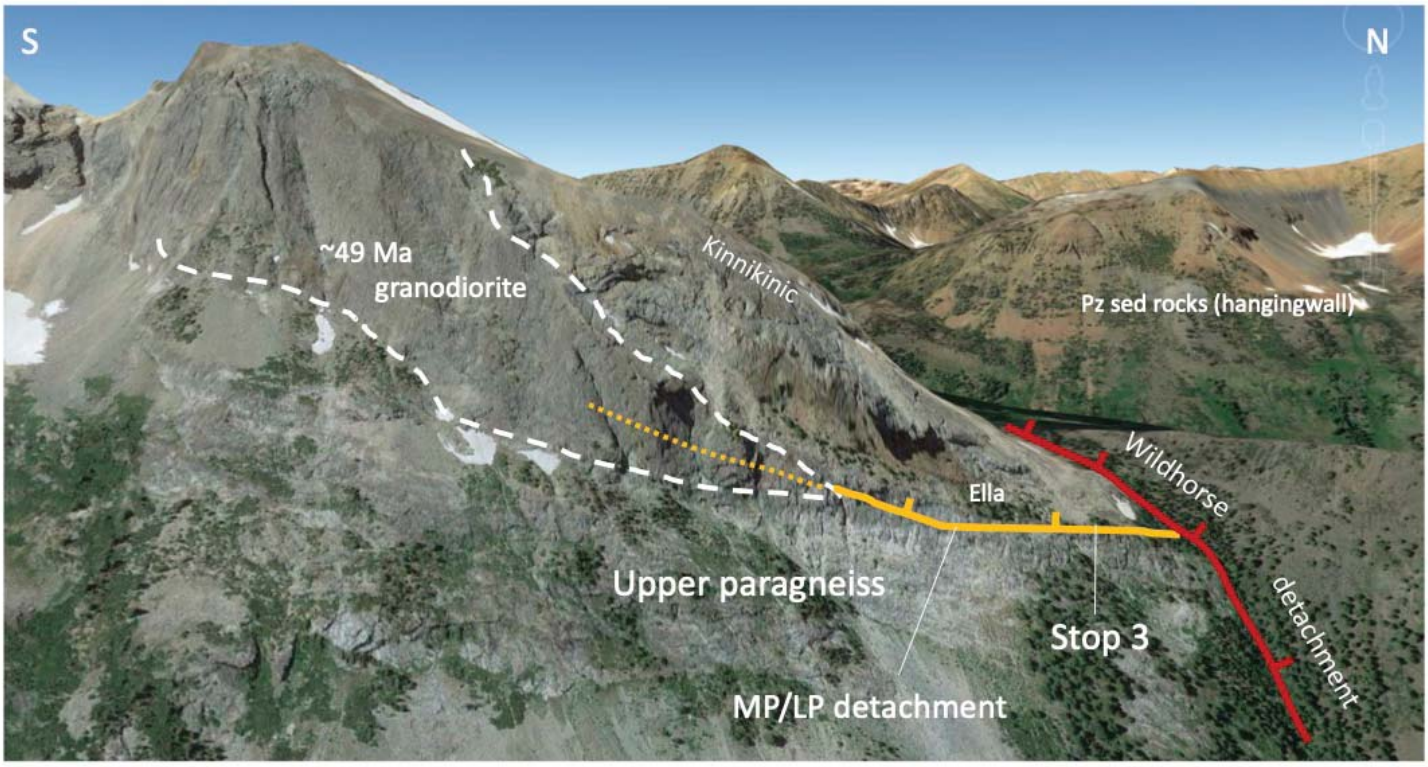

Figure 4. Annotated Google Earth view of field trip area viewed from the east.

STOP 4 43.801167°/-114.187233°

Mylonite Blocks in Granodiorite

This section of outcrops exposes a section of strongly lineated and foliated quartzite with injections of granodiorite. Dover (1983) mapped the quartzite as the upper paragneiss of the lower plate, which would indicate that we are in the MP/LP detachment zone here. At this locality, one can observe isolated blocks of highly lineated mylonitic quartzite largely enclosed within weakly lineated/foliated granodiorite (fig. 6). Lineations in the blocks have variable, but generally WNW to NW trends, suggesting that they are screens of host rock that are generally in their original orientation. In other parts of the outcrop area, the granodiorite is highly strained along with the host quartzite. The amount of strain and fabric development in the granodiorite is highly variable throughout this section.

These relationships suggest that some motion on the MP/LP detachment pre-dated emplacement of the granodiorite, but continued locally after crystallization. The granodiorite yielded a U-Pb zircon crystallization age of 49.2 ± 0.2 Ma (Borel and Vogl, unpublished data).

STOP 5 Optional—Time Permitting

Strained Ordovician Ella–Kinnikinic and Banded Calc-Silicate

This large outcrop provides additional views of mylonitic well-lineated Kinnikinic Quartzite and highly strained Ella marble. Additionally, there is an outcrop of highly deformed banded calc-silicate of the middle plate (Dover's map unit Ybc). The calc-silicate and Clayton Mine Quartzite here appears to be juxtaposed with the Kinnikinic–Ella along a small fault.

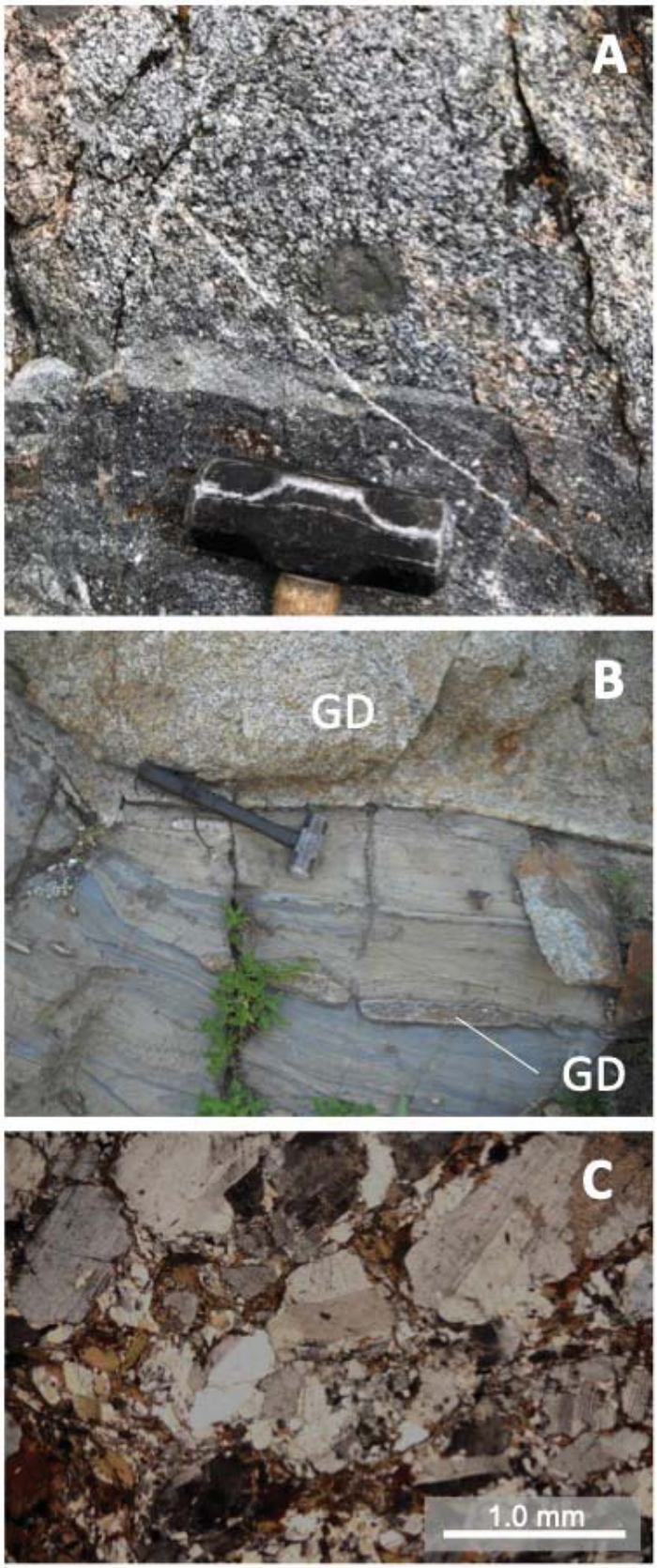

Figure 5. Outcrop photos from MP/LP detachment area at Stop 3. (A) Granodiorite boudins in Ella marble directly overlying the granodiorite. Boudins (labeled GD) include >meter-scale one at the top and smaller elongate ones below. (B) Granodiorite at contact displaying weak protomylonitic fabric. (C) Photomicrograph of granodiorite with protomylonitic textures: quartz subgrains and undulatory extinction, biotite wrapping around feldspar clasts, minor brittle fractures in feldspar.

Figure 6. Photo of well-lineated mylonitic blocks with weakly deformed granodiorite from Stop 4. Granodiorite yielded a U-Pb zircon age of 49.2 ± 0.2 Ma (Borel and Vogl, 2020).

REFERENCES

Borel, M., and Vogl, J., 2020, From brittle to ductile: The relationships between footwall faults, magma emplacement, and its associated heat, Pioneer Metamorphic Core Complex, ID: GSA Abstracts with Programs, v. 52, no. 6.

Brennan, D.T., Pearson, D.M., Link, P.K., and Chamberlain, K.R., 2020, Neoproterozoic Windermere Supergroup near Bayhorse, Idaho: Late-stage Rodinian rifting was deflected west around the Belt basin: Tectonics, 39, e2020TC006145, doi:10.1029/2020TC006145.

Cameron, A., 2010, Geochronology of the lower Wildhorse gneiss complex, Pioneer Mountains, Custer County, Idaho: B.S. thesis, Idaho State University, 43 p.

Diedesch, T.X., 2011, Kinematic analysis of the Wildhorse detachment fault system, Pioneer Mountains, south-central Idaho: M.S. thesis, Idaho State University.

Dover, J.H., 1983, Geologic map and sections of the central Pioneer Mountains, Blaine and Custer counties, Central Idaho: U.S. Geological Survey Miscellaneous Investigations Map I-1319, scale 1:48,000.

Durk-Autenreith, K., 2007, Geochronology of part of the Wildhorse gneiss complex, Pioneer Mountains, Custer County: B.S. thesis, Idaho State University, 38 pp.

Link, P.K., Autenrieth-Durk, K.M., Cameron, A., Fanning, C.M., Vogl, J.J., and Foster, D.A., 2017, U-Pb zircon ages of the gneiss complex of Wildhorse Creek, Pioneer Mountains, south-central Idaho, and tectonic implications: Geosphere, v. 13, p. 681–698, doi:10.1130/GES01418.1.

McFadden, R.R., Mulch, A., Teyssier, C., and Heizler, M., 2015, Eocene extension and meteoric fluid flow in the Wildhorse detachment, Pioneer metamorphic core complex, Idaho: Lithosphere, v. 7, no. 4, p. 355–366, doi:10.1130/L429.1.

O'Neill, R.L., and Pavlis, T.L., 1988, Superposition of Cenozoic extension on Mesozoic compressional structures in the Pioneer Mountains metamorphic core complex, central Idaho: Geological Society of America Bulletin: v. 100, p. 1833–1845.

Ortiz-Guerrero, C., Vogl, J.J. and Foster, D.A., 2020, Accommodation of Eocene crustal extension through isostatically-induced decoupled crustal flow, in the Pioneer Mountains Metamorphic Core Complex (Idaho-US): Geological Society of America Abstracts with Programs.

Silverberg, D.S., 1990, The tectonic evolution of the Pioneer metamorphic core complex, south-central Idaho: Ph.D. thesis, Massachusetts Institute of Technology, 279 p.

Vogl, J.J., Foster, D.A., Fanning, C.M., Kent, K.A., Rogers, D.W., and Diedesch, T., 2012, Timing of extension in the Pioneer metamorphic core complex with implications for the spatial-temporal pattern of Cenozoic extension and exhumation in the northern U.S. Cordillera: Tectonics, v. 31, 22 p., TC1008, doi:10.1029/2011TC002981.

Vogl, J.J., Min, K., Carmenate, A., Foster, D.A., and Marsellos, A., 2014, Miocene regional hotspot-related uplift, exhumation, and extension north of the Snake River Plain: Evidence from apatite (U-Th/He) thermochronology: Lithosphere, v. 6, p. 108–123, doi:10.1130/L308.1.

Wust, S.L., 1986, Extensional deformation with northwest vergence, Pioneer core complex, central Idaho. Geology: v. 14, p. 712–714.